Transport and Communications Science Journal, Vol. 77, Issue 09 (11/2026), 1291-1305

Transport and Communications Science Journal

PATTERN-AWARE FLOOR-TILE LAYOUT OPTIMIZATION AND SCHEDULE-CONSTRAINED OFF-CUT REUSE IN MULTI-ROOM BUILDINGS

Nguyen Thi Thu Hao[1,2], Vo Le Ngoc Dien[3], Doan Dinh Thien Vuong[1,2*]

[1]Faculty of Civil Engineering, Ho Chi Minh City University of Technology (HCMUT), 268 Ly Thuong Kiet Street, Dien Hong Ward, Ho Chi Minh City, Vietnam

[2]Vietnam National University Ho Chi Minh City, Vo Truong Toan Street, Linh Xuan Ward, Ho Chi Minh City, Vietnam

[3]College of Engineering, Can Tho University, Campus II, 3/2 Street, Ninh Kieu Ward, Can Tho City, Vietnam

ARTICLE INFO

TYPE: Research Article
Received: 13/07/2026
Revised: 10/11/2026
Accepted: 12/11/2026
Published online: 15/11/2026
https://doi.org/10.47869/tcsj.77.9.12
* *Corresponding author*
Email: vuong.doanhcmut@hcmut.edu.vn; Tel: 0856141023

Abstract. Tile cut away at room edges wastes material and embodied carbon, yet layout optimizers treat one pattern in one room. This paper develops a two-dimensional layout and packing algorithm: four laying patterns obey a minimum-cut rule, off-cuts are reused across rooms only along precedence-feasible tiling orders searched by simulated annealing, and layouts are compared on waste, cutting effort and an embodied-carbon indicator. Geometry can be read one-way from an Industry Foundation Classes (IFC) model and the indicator covers the tile only, so the framework is neither a complete building information modelling workflow nor a life-cycle assessment. On five computational benchmarks with one tile product per dwelling, default setting-out, a 10 cm minimum cut and nominal joint-free dimensions, reuse lowers the waste of running bond by 53%, and schedule-constrained cross-room reuse lowers waste by 24% and 70% relative to within-room reuse in six- and eight-room apartments (median 37% over 60 random apartments); simulated annealing matched enumeration wherever possible (non-trivially only for six rooms). The eight-room value is a favourable case, because its spans let off-cuts fit later pieces exactly. With 2-3 mm joints and a 2.5 mm kerf the gains are 20-21% and 13-15% (median 28-29%); when as-built span deviations, separate wet-area tiles and one rejected off-cut in five are added, they average 16-17% and 10-18%. Reuse also assumes one production lot; site validation is future work.

Keywords: floor tile layout, off-cut reuse, construction sequencing, multi-objective optimization, construction waste, simulated annealing.

@ 2026 University of Transport and Communications

1. INTRODUCTION

Construction is among the most material-intensive of human activities, and floor finishing contributes a persistent, largely avoidable share of its waste: every tile that meets a wall, a column or a service shaft must be cut, and the off-cut is usually discarded. Procurement estimates therefore rely on industry benchmarks that add 10-20% to the net tiled area [1], a premium that is paid twice - once in money and once in the embodied carbon of manufacturing, transporting and landfilling tile that never serves the building.

The problem is directly relevant to Vietnam, where rapid urbanization generates growing flows of construction and demolition waste [2]; in Hanoi an estimated 40-50% of this waste is landfilled without treatment or recycling, and concrete, clay brick and soil-like material make up more than 80% of the waste dumped at its landfills [3]. At the same time, Building Information Modelling (BIM) is spreading in Vietnamese practice, from infrastructure projects [4,5] to frameworks for BIM-based quantity take-off on high-rise building projects [6], which supply the digital models on which an automated tile-layout optimization can operate. Tiling itself is governed by TCVN 9377-1:2012 [7], whose rules on cut tiles, the laying pattern and the laying order are used in Sections 2.2 and 2.5; the tiles themselves are covered by TCVN 13113:2020 [8], identical to ISO 13006:2018.

BIM makes the geometric part of this problem exactly solvable. Ergen and Bettemir [9] showed that a semantic analysis of the slabs, columns and walls of an Industry Foundation Classes (IFC) model yields an exact floor-covering quantity take-off and an optimal grid layout that minimizes waste in a room, building on ontological algorithms for exact take-off of reinforced-concrete items [10] and on the open IFC data standard, ISO 16739-1 [11]. A parallel line of work optimizes tile layout itself: Wu et al. coupled BIM with parametric design for automated and multi-objective floor-tile planning [1,12], and Xu et al. proposed a generic goal-oriented design method for the layout and cutting of floor tiles [13]. Three gaps remain across these studies. First, each optimizes a single laying pattern - almost always the plain grid - although running bond, one-third offset and herringbone dominate practice and change the cutting geometry entirely. Second, off-cut reuse, where treated at all, is confined to one room or assumed to flow freely between rooms, ignoring the construction schedule that decides whether a leftover piece physically exists when a later room needs it. Third, environmental impact is discussed qualitatively; no study carries an embodied-carbon term calibrated to an environmental product declaration (EPD) inside the objective function; for a single product such a term reduces to a conversion of waste (Section 2.4).

This paper addresses these gaps with a two-dimensional layout, packing and scheduling algorithm whose core contributions are (i) and (iii). (i) A pattern-aware layout engine lays grid, running-bond, one-third-offset and geometric herringbone courses, the herringbone as clipped planks rather than an area allowance, with a field-shift search that enforces a minimum-cut (buildability) rule; its cutting and laying rules follow TCVN 9377-1:2012 [7]. (ii) Layouts are compared on waste, cutting effort and a buildability penalty, with the embodied carbon of the tile as an indicator calibrated to a product EPD under EN 15804+A2 [14]; the criteria can be scalarized or searched by an NSGA-II Pareto optimizer [15,16]. (iii) Cross-room off-cut reuse is made schedule-feasible: a precedence graph restricts off-cuts to rooms tiled later, and a simulated-annealing (SA) scheduler [17] searches construction orders, audited by exhaustive enumeration and a provable area lower bound. (iv) Waste is defined and decomposed explicitly; robustness is examined by Monte-Carlo analysis, a Sobol variance decomposition [18,19] and checks of joints, kerf and site factors; and the predicted waste factors are compared with

published values [1,9] for plausibility. The IFC model is only a one-way geometric input, and the carbon indicator is not a life-cycle assessment (Sections 2.1, 2.4).

Section 2 presents the methodology and the governing equations; Section 3 defines five computational benchmarks; Section 4 reports the results, their robustness and the limitations of the model; Section 5 concludes.

2. METHODOLOGY

2.1. Geometric input and exact quantity take-off

The framework begins where the baseline solver [9] ends: an IfcSlab, the IfcColumn and IfcWall entities bounding it, and any IfcOpeningElement voids can be read with the open-source IfcOpenShell toolkit, and the net tiling region is recovered as a rectangle with rectangular obstacles. Fig. 1 summarizes the architecture. For a room of clear span X × Y tiled with a tile of plan size $w_t \times l_t$, the edge remainders r_x and r_y that force cutting are

$$r_x = X - \lfloor \frac{X}{w_t} \rfloor w_t, \quad r_y = Y - \lfloor \frac{Y}{l_t} \rfloor l_t \tag{1}$$

and every quantity in the paper - tile counts, cut pieces, waste areas - follows deterministically from the room geometry.

Role of the IFC model. The model is only a one-way geometric input: its entity classes identify the slab, walls, columns and openings without layer conventions, so the take-off can be repeated when the design changes, but for rectangular rooms the extracted data equal those of a well-structured CAD drawing (DWG/DXF). The benchmarks of Section 3 are therefore specified by their dimensions, from which all reported results are computed. Property sets, room and door relations, schedule data (IfcWorkSchedule/IfcTask), write-back of the layout (e.g. as IfcCovering elements) and shop drawings are not used (Section 4.9).

2.2. Pattern-aware layout and buildability

Real floors are rarely laid on a plain grid. The engine therefore generates each course j with a per-row horizontal offset o_j that encodes the laying pattern, combined with a global field shift (s_x, s_γ). For each axis three positions are examined (corner start, opposite-corner start and centred cuts), giving nine candidates; the offset of course j is

$$o_j = (s_x + \varphi(j)) \bmod w_t, \ \varphi_{grid} = 0, \ \varphi_{1/2} = \frac{w_t}{2}(j \bmod 2), \ \varphi_{1/3} = \frac{w_t}{3}(j \bmod 3) \tag{2}$$

A true geometric herringbone is laid as 45° interlocking planks clipped at the walls, not as an area allowance. Cut pieces $c \in \mathcal{C}$, of plan size $w_c \times h_c$, whose short side falls below the minimum dimension s_{min} = 10 cm adopted for sound bedding (basis given below) are flagged fragile, and the layout is penalized through

$$\Pi_{sliver} = \sum_{c \in \mathcal{C}} max\left(0, 1 - \frac{min(w_c, h_c)}{s_{min}}\right) \tag{3}$$

The default layout starts at a room corner; when it produces a fragile piece, the candidate with the fewest fragile pieces (then the least waste) is selected, which is how an experienced tiler nudges the first course on site. These nine candidates are used in all case studies; the sensitivity check below, the shifted 60 cm layout of Section 4.2, the best-shift comparisons of Sections 4.1 and 4.4 and the Pareto search of Section 4.5 instead use an exhaustive search over field shifts in 5 cm steps.

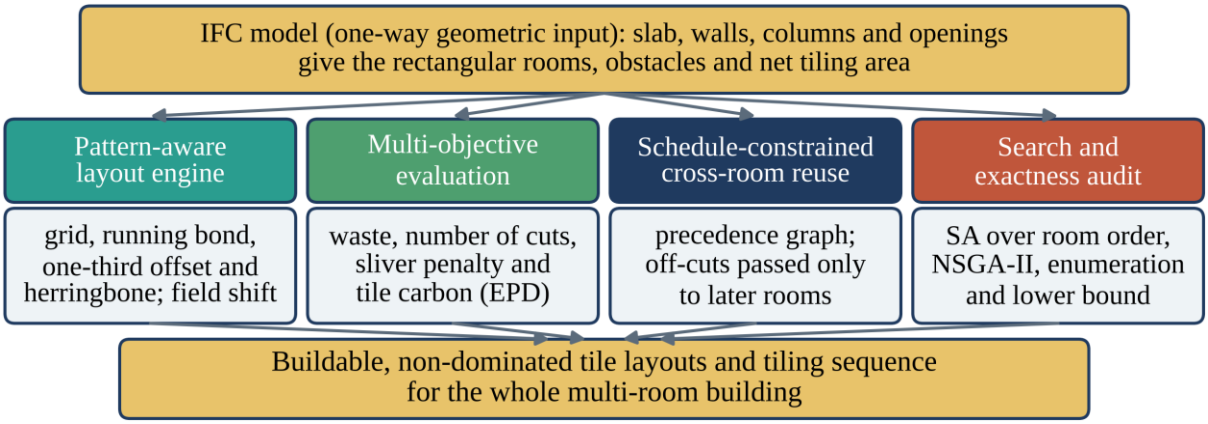


Figure 1. Proposed tile-layout and off-cut reuse framework; the IFC model is a one-way geometric input (SA: simulated annealing; EPD: environmental product declaration).

Basis of the 10 cm minimum cut. TCVN 9377-1:2012 [7] requires cut tiles to have clean cut lines and flat, even joints (cl. 4.1.3.5) and the tiles to follow the designed pattern (cl. 4.2.1.5), but does not specify a minimum width for cut tiles, and the product standard TCVN 13113:2020 [8] does not concern installation. The value s_{min} = 10 cm is therefore a modelling parameter: narrow strips are difficult to bed fully and prone to cracking, so 10 cm (one-sixth of the 60 cm module) is adopted as a conservative value. Off-cuts narrower than s_{min} are scrap, because they can only yield inadmissible pieces. A sensitivity check (s_{min} = 5-20 cm) shows that a single room meets stricter thresholds by a field shift in 5 cm steps without extra waste but with more cuts (CS2, 60 cm tile: 27 instead of 17), whereas the multi-room gain is unchanged in CS3 for s_{min} = 7.5-20 cm but not in CS5 (Section 4.4).

2.3. Off-cut reuse as a two-dimensional cutting-stock problem

Whenever a wall or an obstacle forces a cut, the leftover piece is retained in a pool of reusable off-cuts. Deciding how many brand-new tiles are genuinely needed is then a two-dimensional cutting-stock question [20], closely related to the nesting of pieces on rectangular material sheets [21]: the required cut rectangles are nested into whole tiles by a best-fit decreasing (BFD) guillotine heuristic (pieces in decreasing order of size, each cut from the best-fitting off-cut) that mirrors how a tiler scores a tile and snaps it into two usable parts. The number of new tiles and the packing efficiency are

$$n_{new} = BFD(\{(w_c, h_c)\}_{c \in C}, w_t, l_t), \quad \eta = \frac{\sum_c a_c}{n_{new} A_t} \tag{4}$$

where c ranges over the cut pieces, n_{full} is the number of uncut tiles, a_c the installed area of cut piece c and $A_t = w_t\, l_t$ the tile area; the material actually wasted is the difference between all tile area consumed and the area genuinely covered, A_{cov}:

$$W_{waste} = (n_{full} + n_{new})A_t - A_{cov}, \quad A_{cov} = n_{full}A_t + \sum_{c \in C} a_c \tag{5}$$

Representation and checking of off-cuts. In the rectangular patterns every required piece c is an axis-aligned rectangle ($w_c \times h_c$) in the frame of its parent tile, and every off-cut is kept as a free guillotine rectangle ($f_w \times f_h$); a piece can be cut from an off-cut if it fits with either orientation ($w_c \le f_w$ and $h_c \le f_h$, or rotated), and the best-fitting off-cut (smallest residual area) is chosen. Pieces cut around a column or shaft are sourced from their bounding rectangle, which is conservative. In the herringbone, wall-clipped planks are triangles or trapezoids; each piece

and each off-cut is stored as an exact polygon in the plank frame, and a piece may be cut from an off-cut only if the polygon, as laid or rotated by 180°, lies entirely inside the off-cut (polygon containment test). Each off-cut is reused at most once and flipping glazed planks is not allowed; joints and kerf are neglected except in the checks of Section 4.8, which add the joint width to the tile module, subtract it from every cut piece and remove a 2.5 mm kerf per cut.

Definition of waste. Three quantities are distinguished. (a) Cut-off material is the tile area removed when pieces are cut, including notches around obstacles; without reuse it equals the waste of conventional practice, in which every cut consumes a new tile. (b) Reusable off-cuts are cut-offs whose sides are not smaller than s_{min}; they are returned to the pool and may supply later pieces. (c) Final waste, eq. (5), is all purchased tile area that is not installed: scrap (cut-offs narrower than s_{min} and notches around obstacles) plus reusable off-cuts still unused at the end of the job. Waste factors are expressed as a percentage of the net tiled area A_{cov} (clear floor area minus columns and shafts). Four reference strategies are compared: B0 no reuse; B1 within-room reuse; B2 cross-room reuse in the best unconstrained order; B3 cross-room reuse restricted to precedence-feasible orders. All four use the default setting-out of Section 2.2.

2.4. Multi-objective formulation and embodied-carbon indicator

Each candidate layout is evaluated on four criteria. The embodied carbon of the tile is computed as an indicator with a transparent module-based model aligned with EN 15804+A2 and EN 15978 [14,22]: a cradle-to-gate manufacturing factor (modules A1-A3) and a delivery allowance (A4) apply to all purchased tile, a per-cut energy term covers wet-saw work on site (A5), and a disposal allowance (C2-C4-type factors) applies to the wasted fraction only; as in EN 15978, all burdens of the tile wasted during installation belong to module A5:

$$C = (EF_{mat} + EF_{tr})A_{cons} + e_{cut}n_{cut} + EF_{w}W_{waste} \quad (6)$$

Here A_{cons} is the purchased tile area and W_{waste} the final waste of eq. (5). EF_{mat} is calibrated to a named commercial product, the Mirage ReSource recycled-content porcelain stoneware (8 mm), whose third-party EPD (EPDItaly, 2023) reports a cradle-to-gate global warming potential (GWP-total) of 6.30 $kgCO_2e$ for the declared unit of 1 m² (18.47 kg); no EPD of a tile made in Vietnam was available to the authors, so this value serves as a proxy. Delivery (400 km by road) and disposal (50 km haul, inert landfill) are representative values derived from the same areal mass, and the saw energy assumes a 1.5 kW wet saw running ≈20 s per cut at 0.681 $kgCO_2e$/kWh, Vietnam's 2024 grid emission factor estimated by Hanoi University of Science and Technology with the Ministry of Agriculture and Environment, raised to 0.010 $kgCO_2e$ per cut for blade wear and pumping (Table 1). The factors other than A1-A3 are the authors' representative assumptions, tested in Section 4.6, and any project can substitute its own EPD.

Scope of the indicator. C covers the tile only; the other parts of module A5 (adhesive or bedding mortar, grout, packaging waste and cutting slurry) are excluded, so C is not a life-cycle assessment of the floor. For one product, eq. (6) is affine in waste and cuts, $C = (EF_{mat} + EF_{tr})A_{cov} + (EF_{mat} + EF_{tr} + EF_{w})W_{waste} + e_{cut}\, n_{cut}$, so minimizing C amounts to minimizing waste with a small weight on cuts; carbon becomes a separate criterion only when products with different EPDs are compared. Bedding mortar or adhesive scales with the tiled area and grout with the joint length, so adding them would hardly change the ranking of layouts of one format but would shift the format comparison of Section 4.5. With weights α_i and normalizing reference values C_0 and n_0, the objective vector and the weighted scalarization are

$$min_{p,\sigma} \quad F = [W_{waste}, C, n_{cut}, \Pi_{sliver}] \quad (7)$$

$$Z = \alpha_1 \frac{W_{waste}}{A_{cov}} + \alpha_2 \frac{C}{C_0} + \alpha_3 \frac{n_{cut}}{n_0} + \alpha_4 \Pi_{sliver}, \quad \sum_i \alpha_i = 1 \tag{8}$$

where p denotes the layout decision (tile format, pattern and field shift), σ the tiling order, n_{cut} the number of cuts and Π_{sliver} the buildability penalty of eq. (3).

Table 1. Emission and model parameters (A1-A3 calibrated to a product EPD; other modules representative).

Parameter	Value	Note (EN 15978 module)
Material EF_{mat}	6.30 $kgCO_2e/m^2$	A1-A3 GWP-total, product EPD (EPDItaly, 2023)
Transport EF_{tr}	0.70 $kgCO_2e/m^2$	A4: 18.47 kg/m² × 400 km × 0.095 $kgCO_2e/(t \cdot km)$
Cut energy e_{cut}	0.010 $kgCO_2e$/cut	A5: 1.5 kW × 20 s × 0.681 $kgCO_2e$/kWh (Vietnam grid, 2024) + blade wear and pumping
Waste disposal EF_w	0.40 $kgCO_2e/m^2$	A5, disposal of installation waste (C2-C4-type factors): 18.47 kg/m² × 21.7 $kgCO_2e$/t
Minimum cut s_{min}	10 cm	Modelling parameter; Section 2.2
Breakage probability p_b	3%	Modelling assumption; Section 2.6

2.5. Schedule-constrained cross-room reuse

At building scale an off-cut produced in one room can serve another - but only if the donor room is tiled first. The construction sequence is encoded as a precedence graph G = (V, E) over the rooms, and reuse is restricted to flow forward along any topological order σ, so that room v draws only on the pool P_v of the off-cuts R_u produced in rooms tiled before it:

$$\sigma(u) < \sigma(v) \quad \forall (u,v) \in E, \quad \mathcal{P}_v = \bigcup_{\sigma(u)<\sigma(v)} R_u \tag{9}$$

Because the saving attached to an order depends on the entire accumulated off-cut pool, the ordering problem is sequence-dependent in the sense of the travelling-salesman family and NP-hard in general; exhaustive evaluation costs n! schedule replays, 3.6×10^6 at ten rooms. A simulated-annealing scheduler [17] searches precedence-feasible orders by swapping room pairs, accepting worse moves with the classical probability and geometric cooling:

$$P_{accept} = min\left(1, exp\left(-\frac{\Delta Z}{T_k}\right)\right), \quad T_{k+1} = \gamma T_k, \quad 0 < \gamma < 1 \tag{10}$$

where ΔZ is the change in the objective caused by a swap and T_k the temperature at iteration k.

Definition of the precedence constraints. An edge (u, v) means that room u must be tiled before room v. In CS5 the edges are derived from the access topology of the plan (which room is reached through which) and oriented by TCVN 9377-1:2012 [7] (cl. 4.2.1.5), which sets the general laying direction of a building from the inside outwards; in CS3 they are hypothetical site constraints chosen to test the scheduler: the bathroom, whose waterproofing is completed first, precedes the adjoining kitchen and hall, and the living room precedes the kitchen and both bedrooms, an order that does not follow the inside-out rule. The graphs used are listed in Section 3. A schedule is feasible only if it is a topological order of the graph: the search starts from Kahn's topological sort, rejects any swap that violates an edge, and transfers off-cuts only forward in time.

Search settings and exactness. For fixed layouts, Z in eq. (8) increases linearly with the final waste, so the scheduler minimizes the waste of the order, and ΔZ in eq. (10) is taken as the change in waste (m²). Simulated annealing uses $T_0 = 1.0$ m², $\gamma = 0.9985$, 3000 iterations and a pair-swap neighbourhood; each candidate order is evaluated by replaying the BFD pool. Two levels of exactness must be distinguished. The order is exact only when all precedence-feasible orders are enumerated (here up to eight rooms, by depth-first search with bounding); the BFD packing inside each evaluation is a heuristic, so "exact" refers to the order for the given layouts and packing rule, not to a global optimum of the full layout problem. A provable lower bound, $W_{LB} = (n_{full} + \lceil \Sigma_c w_c h_c / A_t \rceil) \times A_t - A_{cov}$, valid for any cutting plan, is used to certify the gap of larger instances.

2.6. Pareto search, robustness and global sensitivity

Instead of fixing the weights of eq. (8), an NSGA-II genetic optimizer [15] searches the joint space of tile size, pattern and field shift with buildability imposed as a constraint ($\Pi_{sliver} = 0$), ranking solutions on the other three objectives by Pareto dominance,

$$x_1 \prec x_2 \iff F_i(x_1) \le F_i(x_2) \quad \forall i \quad and \quad \exists j: F_j(x_1) < F_j(x_2) \tag{11}$$

and monitoring convergence through the hypervolume dominated by the population [16]. Two stochastic effects are propagated by Monte-Carlo sampling: each required cut is a Bernoulli trial that breaks the tile with probability p_b, consuming an extra tile,

$$\tilde{n}_{cons} = n_{cons} + \sum_{c \in C} B_c, \quad B_c \sim Bernoulli(p_b), \quad \tilde{W} = \tilde{n}_{cons} A_t - A_{cov} \tag{12}$$

where $n_{cons} = n_{full} + n_{new}$ is the number of tiles consumed without breakage and $\tilde{W}$ the waste including breakage; and the two as-built clear spans differ from their nominal values by independent Gaussian deviations (standard deviation 1.5 cm; 3000 samples), which shifts the edge cuts. Monte-Carlo results are reported as the mean together with the 2.5-97.5 percentile range of the simulated outcome (a 95% prediction interval, not a confidence interval of the mean). Finally, a Sobol variance decomposition attributes the variance of the carbon output of the living room of CS5 (Section 3) to six inputs, sampled independently: $EF_{mat} \sim U[5.0, 11.0]$ $kgCO_2e/m^2$ (bracketing the product value, 6.30, and an industry-average porcelain tile), $EF_{tr} \sim U[0.35, 1.40]$ $kgCO_2e/m^2$ (200-800 km), $e_{cut} \sim U[0.005, 0.020]$ $kgCO_2e$/cut, $EF_w \sim U[0.20, 0.80]$ $kgCO_2e/m^2$, $p_b \sim U[0.01, 0.05]$ and the tile size drawn uniformly from seven square formats (30-75 cm). First-order indices are estimated with the estimator of Saltelli et al. applied to the mean-centred output and total-order indices with the Jansen estimator [18,19], from 2^{16} base samples, with 95% bootstrap intervals from 200 resamples.

3. CASE STUDIES

The framework is evaluated on five computational benchmarks, each isolating one mechanism (clear spans in metres; obstacle positions x, y from the corner where tiling starts). CS1 compares four laying patterns, with and without reuse, in a 3.50 × 2.90 room with 60 × 60 cm tiles (herringbone: 60 × 30 cm planks). CS2 contrasts a 120 × 120 cm large-format tile with the 60 cm standard in a 4.70 × 3.70 room containing two columns and a service shaft (0.50 × 0.70 at x = 0-0.50, y = 3.00-3.70; 0.50 × 0.40 at x = 4.20-4.70, y = 0-0.40; 0.60 × 0.60 at x = 2.00-2.60, y = 1.60-2.20). CS3 is a six-room apartment in grid bond with 60 × 40 cm tiles (living 4.20 × 3.60, kitchen 3.35 × 2.85, bed-1 3.85 × 2.85, bed-2 3.35 × 2.35, bath 2.40 × 2.00, hall 3.00 × 1.50; 52.8 m²) with the precedence edges Bath→Kitchen, Bath→Hall, Living→Kitchen, Living→Bed-1 and Living→Bed-2 (Section 2.5). CS4 sweeps twelve catalogue tile sizes

(sixteen cases: the 30 × 60, 40 × 60, 40 × 80 and 45 × 90 cm tiles in both orientations) over 18 zones with spans drawn from {2.60, 3.00, 3.35, 3.85, 4.20, 4.80, 5.40} × {2.00, 2.35, 2.60, 2.85, 3.20, 3.60}, with cross-room reuse in the best order found by simulated annealing (no precedence; 1500 iterations). CS5 is an eight-space dwelling in running bond with 60 × 60 cm tiles (living 5.20 × 4.20 with a 0.60 × 0.60 column at x = 0-0.60, y = 3.60-4.20, kitchen 3.60 × 3.00 with a 0.60 × 0.60 shaft at x = 3.00-3.60, y = 0-0.60, bath-2 2.20 × 1.80, balcony 3.00 × 1.50, corridor 4.80 × 1.40, bed-1 4.20 × 3.60, bed-2 3.60 × 3.30, bath-1 2.40 × 2.00 with a 0.40 × 0.40 shaft at x = 0-0.40, y = 0-0.40; 79.6 m² clear floor, 78.7 m² tiled, ≈85 m² gross including walls). Its graph follows the access topology of the plan, Corridor-{Living, Bed-1, Bed-2}, Living-Kitchen, Kitchen-{Bath-2, Balcony}, Bed-2-Bath-1 (bed-2 is taken as entered from the end of the corridor, which it meets only at a corner in the simplified plan), oriented from the inner rooms to the corridor as required by TCVN 9377-1:2012 (cl. 4.2.1.5) [7]; the opposite, corridor-first orientation is also evaluated. All numbers in Section 4 follow from these definitions, with fixed seeds for all random instances.

4. RESULTS AND DISCUSSION

4.1. Pattern premium and its elimination by reuse

Fig. 2 shows the computed layouts of CS1 in three dimensions. Without reuse, the offset patterns pay a material premium over the grid: running bond wastes 1.37 m² against 0.65 m², because every second course opens two half-tile cuts. Reuse lowers the running-bond waste to 0.65 m² (−53%), and that of the one-third offset falls from 1.73 m² to the same value, so the designer can choose among the rectangular bonds at the waste of the grid (with the best field shift in 5 cm steps, all three reach 0.29 m², the area lower bound). The herringbone remains the cutting-intensive extreme: laid from the corner, its 33 clipped planks (12 of them triangles, none narrower than s_{min}) give a waste factor of 33% without reuse, which the polygon-based reuse of Section 2.3 lowers to 10%.

4.2. Large-format tiles, obstacles and sliver avoidance

CS2 quantifies a trade-off that a waste-only metric hides (Fig. 3). The 120 cm tile needs 10 cuts against 19 for the 60 cm standard laid from the same corner (17 after the field shift of Fig. 3(b)), i.e. far less cutting labour, but its waste factor is 13.6% against 7.0% (4.9% after the shift), and its embodied carbon follows the purchased area upward (132 against 124 $kgCO_2e$). Neither layout contains a piece narrower than s_{min}.

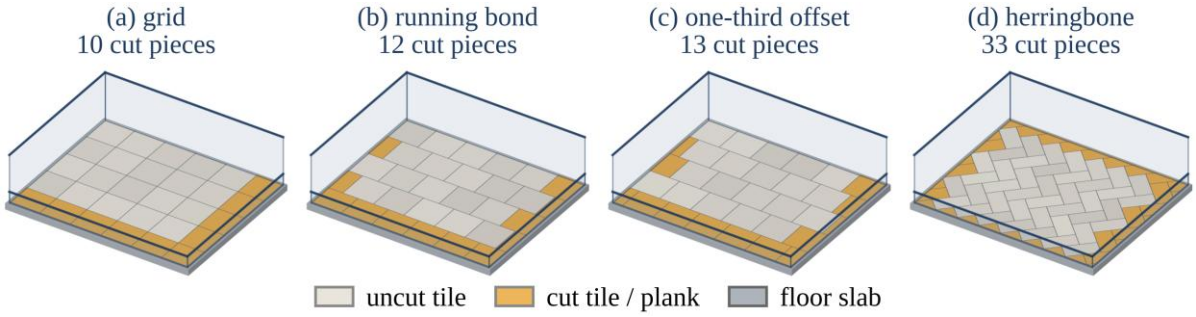


Figure 2. Three-dimensional view of the computed layouts of CS1 on the floor slab: (a) grid, (b) running bond, (c) one-third offset, (d) geometric herringbone of 60 × 30 cm planks; cut pieces shaded.

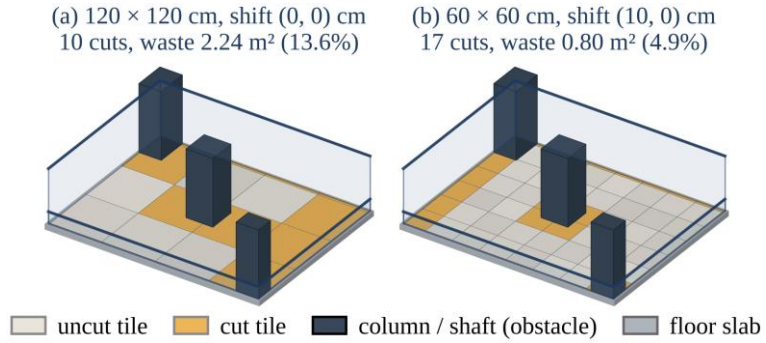


Figure 3. CS2 in three dimensions: (a) 120 × 120 cm large-format layout, (b) 60 × 60 cm layout after the field shift, around two columns and a service shaft; no piece is narrower than 10 cm.

4.3. Schedule-constrained cross-room reuse

Fig. 4(a) separates the four strategies for CS3. Conventional practice (B0) wastes 5.51 m² (10.4% of the tiled area), within-room reuse (B1) 4.07 m² (7.7%), and cross-room reuse 3.11 m² (5.9%) in both the unconstrained (B2) and the precedence-feasible (B3) case, so the construction sequence costs nothing: 24% less waste than B1 and 44% less than B0. The exact optimum is reached by 21 of the 70 feasible orders, e.g. Living → Bed-2 → Bath → Kitchen → Bed-1 → Hall; it reuses 10 off-cuts, and of the final waste, 2.90 m² is reusable off-cuts left in the pool and 0.21 m² is scrap. Carbon falls by 1.8% relative to B1, because purchased material, not cutting, dominates the ledger. In CS4 the best format (60 × 60 cm, 1.89 m²) wastes 75% less than the worst one (30 × 30 cm, 7.47 m²) when rectangular tiles are laid in their better orientation; orientation matters as much (45 × 90 cm tiles: 8.95 or 3.28 m²).

4.4. An eight-room dwelling

CS5 combines the layout, reuse and scheduling steps (Fig. 5). Tiled conventionally (B0; Fig. 4(b)), the dwelling wastes 11.98 m², i.e. 15.2% of the 78.74 m² tiled area (14.1% if referred to the ≈85 m² gross floor area); within-room reuse (B1) reduces this to 1.54 m² (2.0%) and schedule-constrained cross-room reuse (B3) to 0.46 m² (0.6%), a 70% reduction relative to B1 and 96% relative to B0, with 32 off-cuts reused; the final 0.46 m² consists of 0.30 m² of unused off-cuts and 0.16 m² of notches around obstacles. The same optimum is obtained for the inside-out (TCVN) and the corridor-first graph (210 feasible orders each) and without any precedence, and it equals the area lower bound, so it is provably optimal for these layouts; under the inside-out graph every one of the 210 orders reaches it (196 under the corridor-first graph). The large relative reductions, however, reflect a small denominator (the absolute saving relative to B1 is 1.08 m², 1.4% of the floor) and off-cuts that fit later pieces exactly. For s_{min} = 10.5-20 cm, four 10 cm strips become fragile and the shifted layouts give B2 = B3 = 1.18 m² (−23% relative to B1); joints lower the reduction as well (Section 4.8). To test representativeness, 60 random six-room apartments (room sides 1.5-5.6 m; 60 × 60, 60 × 30 or 80 × 80 cm tiles; grid or running bond; four random precedence edges) were solved exactly: the median reduction is 37% relative to B1 (interquartile range 26-62%) and 82% relative to B0 (74-91%). Relative to B1, CS3 (24%) lies near the lower quartile and CS5 (70%) near the 90th percentile, so the two benchmarks bracket the typical case rather than represent it. If the start of each room is also optimized for waste (5 cm steps), within-room reuse alone reaches 0.71 m² in CS3, equal to cross-room reuse, and 1.18 m² in CS5, which cross-room reuse lowers to 0.46 m² (−61%); in the random apartments the median reduction rises to 53% while the median saving halves (2.2% to 1.1% of the floor). Cross-room reuse therefore saves most when the setting-out is fixed by other criteria, such as door thresholds or a centred pattern.

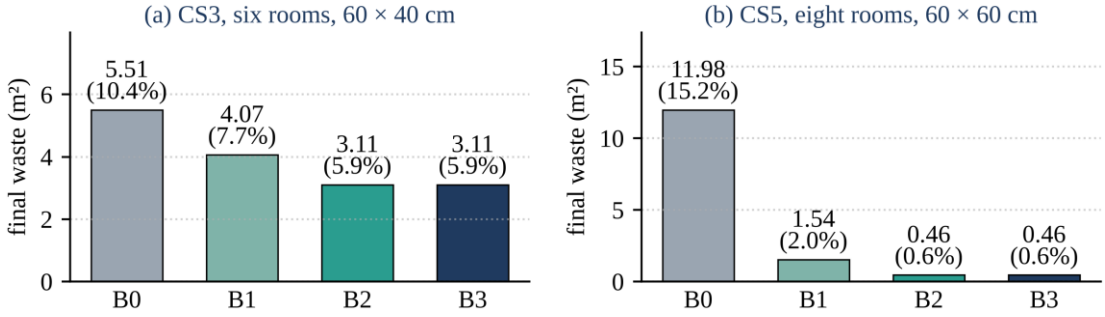


Figure 4. Final waste of (a) CS3 and (b) CS5 under the four strategies: B0 no reuse, B1 within-room reuse, B2 unconstrained and B3 schedule-constrained cross-room reuse; labels give m² and the share of the net tiled area.

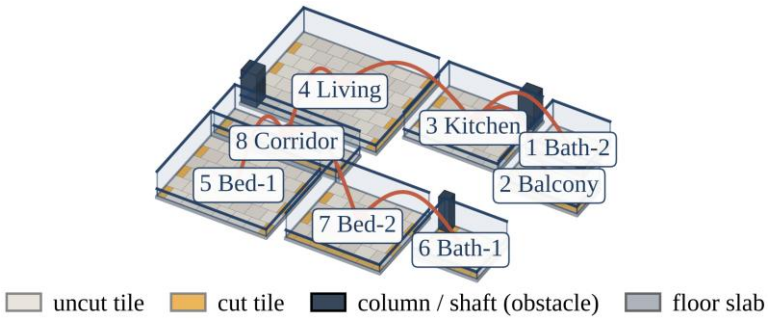


Figure 5. CS5 in three dimensions: an optimal tiling sequence 1-8 (every inside-out order is optimal) and the precedence arcs of the inside-out graph.

4.5. Pareto mapping and exact-optimality audit

Running NSGA-II (integer encoding, population 60, 100 generations) on the CS2 room over the joint space of 17 catalogue formats and orientations (13 tile sizes), three rectangular bonds and field shifts in 5 cm steps maps the trade-off between waste, carbon and cutting effort (Fig. 6). Because one product is used, carbon is affine in waste and cuts (here $C = 115.36 + 7.40\ W_{waste} + 0.01\ n_{cut}$ kgCO₂e; Section 2.4), so the waste-carbon projection is almost a straight line and the front in the three criteria coincides with the waste-cuts front, which is the genuine trade-off. Because this single-room space is small (6,723 candidate layouts, 4,011 of them buildable), it was also enumerated exhaustively. The exact Pareto front contains seven non-dominated points, from 30 × 30 cm tiles (0.17 m², 27 cuts) to the 120 × 120 cm format (2.24 m², 10 cuts), and includes the 60 × 60 cm layout of Fig. 3(b). Over ten seeds NSGA-II recovered five to seven of them and 99.6-100% of the exact hypervolume, reaching 99% after a median of 22.5 generations (range 9-81). NSGA-II thus approximates the front closely but does not certify it. The scheduler was audited on CS3, CS5 (inside-out graph) and random buildings of 8, 12 and 20 rooms (R8, R12, R20: spans as in CS4, 60 × 60 cm tiles, no precedence) with 30 independent runs each (20 for R20, different random seeds). Every run returned the same waste (standard deviation 0), equal to the exhaustive-enumeration optimum for up to eight rooms (30/30 runs). The instances differ in difficulty, however: every feasible order is optimal in CS5 (210 orders) and R8 (40,320 orders, all at the within-room value of 1.38 m²), and in R12 the initial topological order is already the best found, so these cases test stability only; the search is tested by CS3 (21 of 70 orders optimal) and R20, where every run improved the initial order from 4.07 to 3.11 m² and from 2.22 to 1.86 m². For 12 and 20 rooms, where enumeration is impractical, the solution lies 1.3% and 0.9% of the tiled area above the area lower bound, which bounds the remaining optimality gap; a run took 0.11-1.55 s on average.

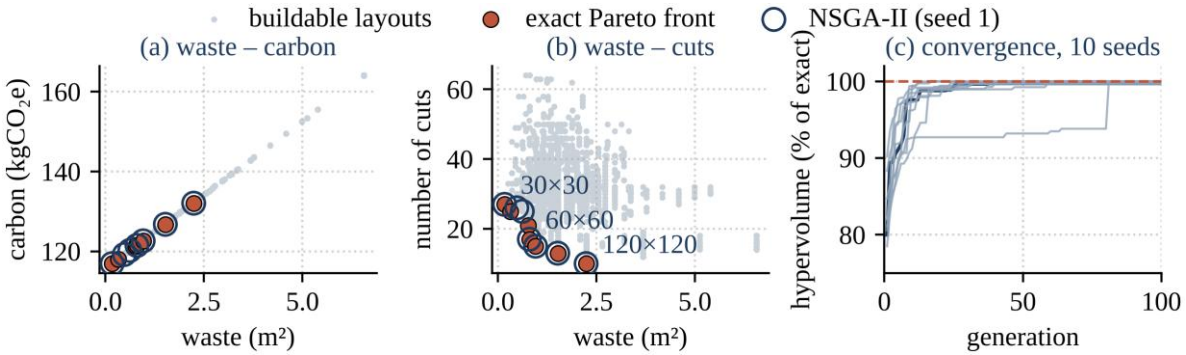


Figure 6. Pareto analysis of the CS2 room: (a) waste-carbon and (b) waste-cuts projections of all buildable layouts, the exact front (enumeration) and the NSGA-II front (seed 1); (c) NSGA-II hypervolume relative to the exact front, ten seeds.

4.6. Robustness and what drives the carbon result

For the living room of CS5 (10 cuts, deterministic waste 0.48 m², 0.36 m² per tile), each cut breaks the tile with p_b = 3%, so the number of broken tiles is binomial: 0 with probability 73.7%, 1 with 22.8% and 2 with 3.2%. Over 10^5 simulations the mean waste is 0.59 m² (exact value 0.48 + 0.36 × 10 × 0.03 = 0.588 m²), the median is 0.48 m² and the 2.5-97.5 percentile range is [0.48, 1.20] m²; the interval is asymmetric because breakage can only add tiles to the deterministic baseline. As-built span deviations matter more. The room depth (4.20 m) is an exact multiple of the tile, so a shorter room cuts the last full row (waste 0.30-0.85 m², 51% of the draws), whereas a longer one opens a sliver row that the field shift removes only by cutting an extra row (2.7-3.2 m², 49%). Without absorption by joints or skirting the outcome is bimodal, with a mean of 1.71 m² and a 2.5-97.5 percentile range of [0.42, 3.06] m²; as-built dimensions should be checked before cutting. In the Sobol analysis, EF_{mat} has a first-order index of 0.94 (95% interval 0.93-0.95) and a total-order index of 0.94 (0.94-0.95), so it acts almost without interaction; it is followed by transport (0.029) and tile size (0.027). The index depends on the assumed range: when the product EPD is known to ±10% it falls to 0.47 and transport (0.33) and tile size (0.20) become comparable, while for an unknown product (4-14 $kgCO_2e/m^2$) it rises to 0.98. EF_{mat} ranks first in every scenario.

4.7. Plausibility check against reported waste factors

Because the benchmarks are computational, Table 2 compares the predicted waste with values reported in peer-reviewed studies [1,9]. This comparison is a plausibility check of magnitude only; it is not a validation, since the published values refer to other rooms, tile formats and practices, not to measurements of the same rooms.

The predicted waste of conventional practice lies inside the 10-20% procurement allowance used as an industry benchmark [1], or slightly above it for the random apartments, which include narrow rooms and 80 × 80 cm tiles; the CS1 grid result lies between the manual and optimized layouts that Ergen and Bettemir [9] report for a similar room (computed from their wastage and spans), and the reductions are of the same order as theirs (Table 2). Vietnam's material norms for cost estimating, by contrast, allow 1.0 m² of tile per m² of floor for every tile size up to 0.54 m² and a 1.0% construction loss for ceramic and porcelain floor tiles (Circular 38/2026/TT-BXD, Appendix VII, items 12.32111-12.32119 and 21.1058); this flat allowance is below the computed waste of conventional practice in every benchmark and is met only by cross-room reuse in CS5 with joint-free geometry (0.6%).

Table 2. Model waste compared with values reported in peer-reviewed studies (waste factors as a percentage of the tiled area; reductions relative to the baseline waste).

Quantity	This study (model)	Reported value
Waste of conventional practice, no reuse (B0)	10.4% (CS3); 15.2% (CS5); median 20.8% over 60 random apartments	10-20% procurement allowance for floor tiles (industry benchmark) [1]
Single room, grid layout	6.4% from the room corner; 2.9% with the best field shift (CS1: 3.5 × 2.9 m, 60 × 60 cm)	≈8% manual, ≈2% optimized with reuse (2.9 × 3.4 m, 30 × 30 cm) [9]
Waste reduction by optimization and off-cut reuse	24-70% vs within-room reuse; 44-96% vs no reuse (CS3, CS5); 13-21% and 39-84% with 2-3 mm joints and kerf	23-73% between best and worst layouts in three of four case studies [9]

4.8. Sensitivity of the reuse gains to joints, dimensions and site conditions

Table 3 recomputes the cross-room gains with the reference assumptions (nominal spans, no joints or kerf, s_{min} = 10 cm, default setting-out, one product, loss-free handling) changed singly or in combination. The 70% of CS5 rests on exact fits: all its spans are multiples of 10 cm, so each of the seven cross-room transfers of the optimum uses an off-cut whole (e.g. the living room's 20 cm off-cuts for the corridor's 20 cm strips) and the 10 cm strips lie exactly at s_{min}. Joints of 2-3 mm turn whole tiles at the walls into near-full pieces with scrap off-cuts and push the 10 cm strips below s_{min}, which changes the setting-out; the optimum then needs only two transfers and saves 0.36 instead of 1.08 m². In CS3 all eight transfers survive with 2.35-3.65 cm to spare (0.96 m² saved with or without joints). With as-built span deviations and joints the CS5 gain varies between 11% and 56% (2.5-97.5 percentiles), so both nominal-span values (70% and 13-15%) are tied to the drawn dimensions. With (b) to (d) combined the mean gains are 16-17% in CS3 (percentiles 5-20%) and 10-18% in CS5 (0-39%; zero for the nominal spans, where the wet-area tile (d) removes the two transfers left by the joints), about 0.5-1 m² per dwelling (random-apartment median 24-28% without (d)); these values, not the joint-free ones, indicate the practical effect. With joints, CS1 (running bond −49 to −50%) and CS2 keep their conclusions, whereas the CS4 format ranking changes (best format: 60 × 60 cm at 2 mm, 40 × 80 cm at 3 mm).

Table 3. Reduction of final waste by cross-room relative to within-room reuse (B3 vs B1) under changed assumptions (span deviations: standard deviation 1.5 cm, 300 samples for CS3 and CS5, 20 per random apartment; Random: median of the 60 random apartments, without (d)).

Condition	CS3	CS5	Random
Reference model (Sections 4.3 and 4.4)	24%	70%	37%
Minimum cut s_{min} = 10.5-20 cm	24%	23%	24-34%
Start of each room optimized (5 cm steps)	0%	61%	53%
(a) 2 / 3 mm joints, 2.5 mm kerf	21% / 20%	15% / 13%	28% / 29%
(b) As (a), with as-built span deviations (mean)	17% / 18%	38% / 32%	29% / 33%
(c) One transferred off-cut in five rejected (mean)	22%	63%	32%
(d) Separate 30 × 30 cm tile in bathrooms and balcony	22%	59%	-
(b), (c) and (d) combined (mean)	16% / 17%	18% / 10%	24% / 28%

4.9. Scope of applicability, assumptions and limitations

The results are computational and rest on stated assumptions. (i) Geometry: rooms are orthogonal rectangles with rectangular obstacles; diagonal or curved walls, L-shaped rooms and thresholds would require polygon clipping of the field and polygon nesting of the pieces, for which the polygon representation of the herringbone (Section 2.3) is the natural basis. (ii) Cutting: pieces around obstacles are sourced from bounding rectangles and herringbone off-cuts are reused only once, which is conservative, whereas joints and saw kerf enter only the checks of Section 4.8. (iii) Site conditions: each dwelling uses one tile product from one production lot, since lots may differ in shade, and in work size within the dimensional tolerances of TCVN 13113:2020 [8]; off-cuts are collected, stored and moved without loss; breakage is an independent 3% per cut, and as-built span deviations are not absorbed by joints or skirting (Section 4.6). Handling is limited: an optimal order needs as few as 8 (CS3) and 7 (CS5) off-cut transfers between rooms, each saving on average about half a tile (0.12 and 0.15 m²), which caps the cost worth spending on handling one off-cut; rejected off-cuts and separate wet-area tiles lower the gains (Table 3). (iv) BIM and scheduling: the IFC model is only a one-way geometric input (Section 2.1), and the precedence graphs are inputs from the access topology and TCVN 9377-1 [7] or, in CS3, from hypothetical site constraints, without storage limits or curing times. (v) Carbon: the indicator covers the tile only and uses one product EPD from outside Vietnam (Section 2.4). (vi) Optimality is certified only for the room order (enumeration or lower bound), not for the BFD packing or the NSGA-II front. (vii) Layouts use the default setting-out of Section 2.2, and the gains refer to s_{min} = 10 cm and nominal joint-free spans (Section 4.8). (viii) No measured site data were available; the literature comparison of Section 4.7 is a plausibility check, and an instrumented pilot project is required before the absolute figures are used for procurement. Within these limits the framework applies to apartments and offices with rectangular rooms tiled in rectangular or herringbone bonds, provided that it is run with as-built dimensions and the actual joint width.

5. CONCLUSION

This paper extended floor-tile layout optimization from a single-objective, single-pattern, single-room exercise to a pattern-aware and schedule-aware algorithm for whole dwellings, with geometry that can be read from an IFC model. Off-cut reuse removes the material premium of offset patterns (−53% for running bond). With nominal joint-free dimensions, default setting-out and a 10 cm minimum cut, schedule-constrained cross-room reuse reaches the unconstrained optimum in both apartments, lowering waste by 24-70% relative to within-room reuse (median 37% over 60 random apartments), so a buildable sequence (TCVN-compliant in CS5) costs essentially no material. The 70% of CS5 is a favourable case in which off-cuts fit later pieces exactly; with 2-3 mm joints and a 2.5 mm kerf the gains are 20-21% and 13-15% (median 28-29%), and when as-built span deviations, separate wet-area tiles and one rejected off-cut in five are added, they average 16-17% and 10-18%. Simulated annealing was stable: it returned the same waste in every run, matched enumeration wherever possible (a discriminating test only in CS3) and stayed within 1.3% of the tiled area of a provable lower bound for 12-20 rooms. For one product the carbon indicator is affine in waste and cuts and governed by the A1-A3 factor of the EPD, so it adds no trade-off of its own.

The study is limited to rectangular geometry, one-way use of the IFC model, a tile-only carbon indicator and computational evidence (Sections 4.8 and 4.9). Future work will validate the predictions and the handling effort on Vietnamese projects, extend the engine to non-

rectangular rooms, write the layout back to the model, read room functions, access and the tiling order from it (IfcSpace, IfcDoor, IfcWorkSchedule/IfcTask) and add adhesive, grout and locally made products to the carbon indicator.

REFERENCES

[1]. S. Wu, N. Zhang, Y. Xiang, D. Wu, D. Qiao, X. Luo, W.-Z. Lu, Automated layout design approach of floor tiles: based on building information modeling (BIM) via parametric design (PD) platform, Buildings, 12, 250, 2022. https://doi.org/10.3390/buildings12020250

[2]. H. T. Nghiem, Q. M. Phan, K. Kawamoto, K. T. Ngo, H. G. Nguyen, T. D. Nguyen, Y. Isobe, M. Kawasaki, An investigation of the generation and management of construction and demolition waste in Vietnam, Detritus, 12 (2020) 135-149. https://doi.org/10.31025/2611-4135/2020.14002

[3]. H. G. Nguyen, D. T. Nguyen, H. T. Nghiem, V. C. Tran, A. Kato, A. Matsuno, Y. Isobe, M. Kawasaki, K. Kawamoto, Current management condition and waste composition characteristics of construction and demolition waste landfills in Hanoi of Vietnam, Sustainability, 13, 10148, 2021. https://doi.org/10.3390/su131810148

[4]. T. T. Ngo, M. T. Do, X. T. Huynh, Overview of BIM application for bridge - highway and infrastructure projects in Viet Nam, Transport and Communications Science Journal, 71 (2020) 760-774. https://doi.org/10.47869/tcsj.71.7.3

[5]. D. D. Nguyen, T. T. Quach, Application of building information modeling in Vietnamese bridge construction, Transport and Communications Science Journal, 72 (2021) 908-919. (in Vietnamese). https://doi.org/10.47869/tcsj.72.8.5

[6]. T.-Q. Nguyen, E. C. W. Lou, B. N. Nguyen, A theoretical BIM-based framework for quantity take-off to facilitate progress payments: the case of high-rise building projects in Vietnam, International Journal of Building Pathology and Adaptation, 42 (2024) 704-728. https://doi.org/10.1108/IJBPA-10-2021-0139

[7]. TCVN 9377-1:2012, Finish works in construction - Execution and acceptance - Part 1: Paving and smoothing works, Ministry of Science and Technology, Hanoi, 2012 (in Vietnamese).

[8]. TCVN 13113:2020 (ISO 13006:2018), Ceramic tiles - Definitions, classification, characteristics and marking, Ministry of Science and Technology, Hanoi, 2020 (in Vietnamese).

[9]. F. Ergen, Ö. H. Bettemir, BIM-driven software and algorithm for optimal floor tile layout minimizing material waste, Automation in Construction, 173, 106115, 2025. https://doi.org/10.1016/j.autcon.2025.106115

[10]. F. Ergen, Ö. H. Bettemir, Development of ontological algorithms for exact QTO of reinforced concrete construction items, Structures, 60, 105907, 2024. https://doi.org/10.1016/j.istruc.2024.105907

[11]. ISO 16739-1:2024, Industry Foundation Classes (IFC) for data sharing in the construction and facility management industries - Part 1: Data schema, International Organization for Standardization, Geneva, 2024.

[12]. S. Wu, N. Zhang, X. Luo, W.-Z. Lu, Multi-objective optimization in floor tile planning: coupling BIM and parametric design, Automation in Construction, 140, 104384, 2022. https://doi.org/10.1016/j.autcon.2022.104384

[13]. Y. Xu, J. Wang, Z. Yang, Generic goal-oriented design for layout and cutting of floor tiles, Automation in Construction, 152, 104903, 2023. https://doi.org/10.1016/j.autcon.2023.104903

[14]. EN 15804:2012+A2:2019, Sustainability of construction works - Environmental product declarations - Core rules for the product category of construction products, European Committee for Standardization (CEN), Brussels, 2019.

[15]. K. Deb, A. Pratap, S. Agarwal, T. Meyarivan, A fast and elitist multiobjective genetic algorithm: NSGA-II, IEEE Transactions on Evolutionary Computation, 6 (2002) 182-197. https://doi.org/10.1109/4235.996017

[16]. E. Zitzler, L. Thiele, Multiobjective evolutionary algorithms: a comparative case study and the strength Pareto approach, IEEE Transactions on Evolutionary Computation, 3 (1999) 257-271. https://doi.org/10.1109/4235.797969

[17]. S. Kirkpatrick, C. D. Gelatt Jr., M. P. Vecchi, Optimization by simulated annealing, Science, 220 (1983) 671-680. https://doi.org/10.1126/science.220.4598.671

[18]. I. M. Sobol', Global sensitivity indices for nonlinear mathematical models and their Monte Carlo estimates, Mathematics and Computers in Simulation, 55 (2001) 271-280. https://doi.org/10.1016/S0378-4754(00)00270-6

[19]. A. Saltelli, P. Annoni, I. Azzini, F. Campolongo, M. Ratto, S. Tarantola, Variance based sensitivity analysis of model output. Design and estimator for the total sensitivity index, Computer Physics Communications, 181 (2010) 259-270. https://doi.org/10.1016/j.cpc.2009.09.018

[20]. P. C. Gilmore, R. E. Gomory, Multistage cutting stock problems of two and more dimensions, Operations Research, 13 (1965) 94-120. https://doi.org/10.1287/opre.13.1.94

[21]. B. D. Tran, T. N. Pham, Optimization of oriented nesting layout on rectangular material sheets, VNUHCM Journal of Science and Technology Development, 13 (2010) 43-50. (in Vietnamese). https://doi.org/10.32508/stdj.v13i3.2133

[22]. EN 15978:2026, Sustainability of construction works - Assessment of environmental performance of buildings - Requirements and guidance, European Committee for Standardization (CEN), Brussels, 2026.